ELSEVIER

Surface Science 382 (1997) 154–169

surface science

Ab initio calculation of molecule-surface binding: methyl halides on GaAs(110) surfaces

S. Black [a,1], R. Friesner [a,*], P. Lu [b], R. Osgood [b]

[a] *Department of Chemistry, Columbia University, New York, NY 10027, USA*
[b] *Columbia Radiation Laboratory, Columbia University, New York, NY 10027, USA*

Received 25 September 1996; accepted for publication 9 January 1997

Abstract

Large scale ab initio cluster calculations are used to examine the binding of methyl halides to the (110) surface of GaAs. The results of the calculations are compared with recent experimental measurements of the binding energies. Three approaches to electron correlation are examined: density functional methods utilizing the generalized gradient approximations (specifically, the BLYP functional) or adiabatic connection formulas (B3LYP), and local MP2 methods which intrinsically eliminate basis set superposition errors. The BLYP calculations are found to underestimate the binding substantially; the B3LYP and LMP2 results are closer to experiment but are still underestimates. Structures optimized at the B3LYP level are in good agreement with experimental geometries. The results are encouraging with regard to the ability of suitable quantum chemical methods to accurately treat the dative bonding important for a reliable description of molecule–surface interactions. © 1997 Elsevier Science B.V.

Keywords: Ab initio quantum chemical methods and calculations; Density functional calculations

1. Introduction

Theoretical understanding of molecule–surface interactions is a major goal of computational materials science. A wide variety of approaches exist for modeling the interaction of small molecules with surfaces, ranging from entirely empirical force fields to high level ab initio quantum chemistry (see for example Refs. [1–4]). In contrast to organic molecules, however, the force fields developed for materials such as semiconductors are of uncertain quality, particularly when considering the difficulty in calculating quantities such as binding energies in which the local electronic structure of the surface can change significantly. Consequently, the development of methods capable of producing benchmark results is crucial to achieving high accuracy.

The logical candidate for carrying out calculations of this quality for complex materials is ab initio quantum chemistry. However, there are formidable problems inherent in the application of quantum chemical methods to surface science. The most significant of these are as follows:

(1) The molecule–surface system is neither periodic nor finite. Therefore, some approximations have to be made in treating the long-range interactions.
(2) High levels of electron correlation are typically required to obtain the desired observables to

* Corresponding author. Fax: +1 212 8547454; e-mail: rich@chem.columbia.edu

[1] Presently at Norfolk State University.

PII S0039-6028(97)00119-2

reasonable accuracy, in some cases to obtain even qualitatively reasonable results.

(3) Modeling of the surface and surface–adsorbate structures presents substantial problems; these are accentuated for weakly bound systems.

In particular, the combined requirements of large systems, accurate electron correlation, and geometry optimization necessitate extremely large requirements for memory and CPU time. Hence, few first principles calculations of molecule–surface binding energies have been carried out and shown to provide a reasonable reproduction of the experimental results.

There are a number of approaches to the above problems which have been developed over the past two decades. One class of methods is based upon solid state density functional methods [5,6], typically employing plane-wave basis sets. Such methods have proven to be reasonably effective for computation of the properties of bulk solids, and there have been some applications to problems such as surface reconstruction and chemisorbed systems. However, the core electronic structure approximation used in these codes was for many years the local density approximation (LDA). As this methodology displays ~ 50 kcal mole^{-1} average errors in small molecule bond energies, it was not possible to obtain quantitative prediction of binding energies.

A major advance in the ability to treat molecule surface interactions using this type of approach was made possible by the work of Becke [7–9] in developing new density functional theory (DFT) methods with qualitatively superior accuracy to that provided by the local density approximation (LDA), which had been used almost exclusively in previous work. Becke has developed two types of new DFT methods: generalized gradient (GGA) functionals, such as the BLYP approach [8], and functionals containing an admixture of Hartree–Fock exchange, such as the B3LYP approach [7]. The excellent performance of these functionals for small molecule bond energies (an order of magnitude improvement in average error as compared to the LDA) suggested that similar accuracy could be achieved in molecule–surface calculations.

Recent work by Nørskov [10] has confirmed that this hypothesis is in fact the case. Using plane-wave DFT methods and a GGA functional, impressive results have been obtained for the binding energy of a number of small molecules to metal surfaces. In comparison with experiment, the accuracy of reported binding energies is typically on the order of 0.1–0.5 eV: this precision is in good accord with Becke's GGA results for the G2 data base of small molecules. For chemisorbed systems, where the total binding energies are ~ 1–2 eV, this is a reasonable level of accuracy and has allowed important qualitative features of molecule–surface binding to be elucidated.

Our interest in this paper, however, is for systems of a rather different type, specifically dative bonding of a molecule on a semiconductor surface. In contrast to chemisorbed systems, the binding energy is significantly weaker, on the order of 0.5 eV. Thus, to achieve a level of accuracy sufficient to differentiate the specifics of molecule–surface chemistry, a higher level of accuracy would be desirable.

The density functionals based upon Hartree–Fock exchange have a superior level of accuracy in the small molecule test suites [7] and hence would be expected to provide improved results in the present case as well. Unfortunately, it is not currently possible to treat such functionals via DFT plane-wave methods due to the requirement for computation of the Hartree–Fock exchange term. Alternatively, one might hope to obtain greater precision using ab initio wavefunction-based methods incorporating high levels of electron correlation; again, plane-wave methods cannot handle this type of calculation.

In order to apply these via alternative electron correlation methods, one must resort to a finite cluster methodology, capping dangling bonds with hydrogen or utilizing some sort of embedding procedure. This is the approach we adopt here. The key to obtaining reasonable results with this approach is the ability to treat a sufficiently large finite cluster (making the edge effects small) while at the same time employing a sufficient level of electron correlation. Our PSGVB ab initio electronic structure code [11] is well suited to this task, having been specifically developed for effi-

ciently carrying out correlated calculations on large systems.

The use of a large cluster, in and of itself, is not sufficient to guarantee reasonable results. The detailed structure of the approximating cluster is of equal importance to its size, as are the types of geometry optimization that are carried out. Consequently, we have studied a series of clusters in an attempt to investigate the dependence of the results upon cluster shape and structure, so as to understand the criteria for obtaining converged results.

There have been a significant number of previous studies of molecule–surface interactions using cluster methods, along with various types of electron correlation [12–16]. Many of these have been restricted to small clusters which, for the type of interactions we investigate here, are inadequate to even qualitatively describe the molecule–surface interaction. To investigate larger systems, some workers have used embedded cluster approaches [12,16] or slab calculations [13]. However, these papers, while evaluating binding energies, in general have not presented direct comparisons of these values with reliable experimental data. It is only in this fashion that the impact of the approximations inherent in any given protocol (cluster size and structure, electron correlation method, basis set) can be evaluated. This is the principal objective of the present paper.

As an initial test case, we study the magnitude of the binding energy and molecular orientation of methyl halides to a GaAs(110) surface. This system has been investigated extensively via angle-resolved time of flight and NEXAFS measurements by Osgood and coworkers [17–19]; in addition, detailed information concerning binding energies and structures are available for isolated methyl halide molecules. While the interaction of methyl halides with GaAs is an important model system for probing optical surface interactions, the primary objective of the present work is to see what level of quantum chemical model is needed to compute realistic structures and interactions. Although the conclusions we emerge with are by no means definitive, they do represent, in our view, significant progress towards an accurate ab initio approach to molecule–surface interactions.

The paper is organized as follows. In Section 2, we briefly describe the theoretical methods and the PSGVB electronic structure code. Section 3 presents results for a series of molecule–surface clusters treated with different electron correlation methods. Section 4, the conclusions, discusses how the methodology used here can be extended and improved.

2. Computational methods

2.1. Overview

The PSGVB program was used for all electronic structure calculations. The program employs traditional contracted Gaussian quantum chemical basis sets, but uses numerical algorithms (pseudospectral methods) originally derived from fluid dynamics simulations to accelerate the calculation of Coulomb and exchange operators. For self-consistent field (SCF) calculations of either the Hartree–Fock (HF) or DFT type, a computational advantage of a factor of $\sim$5–10 in geometry optimizations is typically obtained as compared to conventional ab initio programs, for example Gaussian 92 [20].

We have recently developed a series of correlated electronic structure methods based upon localized molecular orbitals, along the lines proposed by Pulay and coworkers [21]. Using pseudospectral techniques allows full advantage to be taken of the reduction of the virtual space that arises from using only local correlating orbitals. Our PS-LMP2 method scales as $N^{2.5}$ (in contrast to the N^5 observed for conventional MP2 with large basis sets) and yields an order of magnitude advantage in CPU time for a small organic molecule such as piperidine, using the cc-pVTZ correlation consistent basis set of Dunning and coworkers [22]. Furthermore, basis set superposition error is eliminated in localized methods, because the orbitals on one fragment of a complex do not contribute to correlating the internal terms on the second fragment, therefore there is no need for the use of counterpoise correction. This has been documented in detail by Saebo and Pulay for the water dimer [23].

To illustrate the variations in binding energies obtained with conventional and local MP2 for the present class of systems, we consider a model problem in which Ga_4AsH_9 is dissociated into the fragments Ga_3AsH_6 and GaH_3, breaking a dative bond similar to that seen in the adsorbate–cluster systems discussed below. Table 1 presents the results of Hartree–Fock, conventional MP2 calculations with and without the counterpoise correction, and local MP2 results, for the dissociation energy. The HF results are qualitatively in error. As expected, the LMP2 results lie between the uncorrected and corrected conventional MP2 results; based upon the arguments made in the previous paragraph, we expect that the LMP2 results are the most accurate.

A major objective of the present paper is to test several density functional methods with regard to their ability to reliably compute relatively weak molecule–surface interactions. The PSGVB code contains most of the important DFT functionals currently available. Here, we choose to examine the gradient-corrected BLYP method and the B3LYP approach, both based on approaches developed by Becke several years ago [7,8] which have been modified [20] to use the LYP correlation functional [24]. The B3LYP method contains an admixture of Hartree–Fock exchange, and hence cannot be efficiently coded in plane-wave DFT methods (no problems are presented for Gaussian-based ab initio codes). The performance of B3LYP is also qualitatively superior to that of BLYP, yielding an average error in bond dissociation energies for the small molecule G2 data base of 2.4 kcal $mole^{-1}$ as compared to the 5.7 kcal $mole^{-1}$ obtained for BLYP (by contrast, the LDA averages an error of 50 kcal $mole^{-1}$ and hence is expected to be rather useless for binding energies).

Table 1
GaH_3/Ga_3AsH_6: binding energy (kcal mol^{-1})

	PS-GVB	Gaussian 92	Gaussian 92-CP
HF	0.40	0.43	0.19
MP2	3.06	5.56	2.62

2.2. Basis set

In the description of the heavy atoms we used Effective Core Potentials (ECP) and a valence basis sets (33/31), developed at Los Alamos National Laboratory [25]. To this set we added a *d* polarization function, energy-optimized at the experimental geometry of the homonuclear dimers, this being necessary for the recovery of an appreciable fraction of the correlation energy. Exponents for these *d* functions are presented in Table 2. This basis set we call LAV3P*. Hydrogen and carbon were represented by 6–31G** basis sets.

3. Calculation of methyl halide interactions with the GaAs(110) surface

3.1. Overview

3.1.1. Qualitative nature of the GaAs(110) surface

Crystalline GaAs is a tetrahedrally bonded solid, the surface properties of which differ greatly from that of the bulk. GaAs bulk atoms undergo sp^3 hybridization and all four bonds appear indistinguishable, but this symmetry is broken at the surface, with lone pairs localized on the As atoms, and Ga atoms lacking a pair of electrons in their outer shell. Therefore the surface presents both an electron-rich site, ready to participate as a donor in a coordinate covalent bond, and an electron-deficient site, capable of receiving an electron-pair donation. Finally the (110) surface contains a permanent dipole moment aligned from Ga to As, contrasting, for example, with the absence of a large electric dipole in the case of Si surfaces. Note that the GaAs(110) surface relaxes in the process of assuming a different electronic distribution: the As surface atoms move upward in relation to their Ga lateral neighbors, which take a more sp^2-like

Table 2
Optimized polarization functions

	Ga	As	Cl	Br	I
d exponent	0.17	0.28	0.60	0.41	0.28

structure, and the orientation of the bonds shows more resemblance to that of a free molecule. The second and third layers also undergo relaxation, with less pronounced changes from those in the bulk.

3.1.2. Construction of model clusters

In constructing our GaAs clusters, existing experimental data were utilized for the GaAs bulk and for the GaAs(110) surface to provide an initial guess for bond angles and bond lengths of the various atoms. Capping hydrogen atoms were placed at the same angle as the absent Ga or As atom, but the bond distances were changed to the experimental distances of Ga–H or As–H in the Ga and As trihydrides, respectively. Three sizes of clusters were employed and are designated small (three heavy atoms), medium (nine heavy atoms), and large (24 heavy atoms). Two different medium clusters were investigated to examine the effects of altering the cluster structure.

3.1.3. Binding of methyl halides to the GaAs(110) surface

The experimental results [17–19] indicate that the bonding between methyl halides and the GaAs(110) surface lies on the border between chemisorption and physisorption, the dissociation energy of the surface–adsorbate system being of the order of half an electron volt (about 11 kcal mol^{-1}). From this relatively weak interaction, one might a priori expect only small changes in the GaAs(110) surface and bulk structure due to the presence of the adsorbate.

Initial guesses for the cluster–methyl halide complex structure were constructed using chemical intuition. We based our choice on the premise that the most important binding effects would come from the dipole–dipole interaction of the methyl group of the adsorbate with the surface. As atoms directly connected to the Ga binding site and from the transfer of negative charge from the halogen atom to the binding surface Ga atom. Several other adsorbate–surface complexes were investigated, but none yielded total energies as low as the structures we picture here. While this does not constitute definitive proof that the complexes used are the lowest energy minima, we believe that this is very likely on the basis of our results.

3.2. Geometry optimization of clusters and complexes

3.2.1. Methyl halides

As discussed above, the weak nature of the adsorbate–surface interactions suggests that only minor modifications of the GaAs near-surface structure occur upon adsorption of methyl halide molecules; therefore a full scale geometry optimization involving all atoms in the cluster is not necessary. This is fortunate since major distortions of the structure at the edges would occur during the optimization, as the hydrogen capping does not properly constrain the bulk or surface atoms correctly. Consequently, we used, primarily, constrained-geometry optimization, either freezing the cluster or, for the large cluster, allowing the atoms closest to the adsorbate (on the first layer) to move in the $[1\bar{1}1]$ plane while freezing the remainder in the appropriate bulk and surface positions. Also, for the largest cluster, we have included the effects of surface reconstruction, utilizing experimental data to generate an initial guess for the surface geometry and again optimizing the position of those same surface atoms which were allowed to move in the cluster–adsorbate system.

We also present results for the unconstrained geometry optimization of the small cluster to illustrate how poorly such a system describes the stable GaAs surface. In calculating binding energies, the bare cluster, used as a reference, is treated in exactly the same fashion as the complex with regard to the geometrical constraints imposed, otherwise the resultant binding energy would not be meaningful.

3.2.2. Hydrogen halides

In addition to calculations on methyl halides, we have performed similar adsorption calculations for the hydrogen halides. While there is no experimental data for these systems at present, it is useful to contrast the results for the two adsorbate species. Furthermore, if experimental data is generated at a future date, the present results constitute a prediction as to what should be observed.

3.3. Results for various cluster sizes

3.3.1. Small clusters

The principal objective in studying small clusters is to illustrate artifacts that arise from insufficiently large cluster diameters. For example, in such cases the hydrogen atoms directly bonded to the Ga and As atoms near the adsorbate may participate in the adsorbate–surface bonding process. A related consequence of this participation results from the effects on the different electronegativity of H (2.1 eV) on the electronic distribution on the nearby heavy atoms. As mentioned earlier, As and Ga have electronegativities of 2.0 eV and 1.6 eV, respectively, therefore, the As–Ga bond has a dipole moment pointing from the As atom to the Ga atom. When a hydrogen atom is substituted for As, the new H–Ga bond has a dipole moment similar to the original As–Ga one; when Ga is replaced by H, the dipole direction is actually reversed and there is a drawing of charge from As which is not present in the real crystal–adsorbate system.

The validity of constrained geometry optimization when using small clusters to represent the surface was ascertained by comparing results of total geometry optimization of isolated $GaAs_2H_5$ and of the $HBr/GaAs_2H_5$ system to those obtained with the frozen cluster, optimizing just the HBr geometry. As mentioned before, the heavy atoms in the cluster are placed to reproduce the crystal structure; therefore the cluster should not change significantly during the geometry optimization procedure if it is a good representation of the crystal surface. Table 3 presents the binding energy calculated via these two different procedures. The adsorption energy becomes much weaker when all the coordinates were allowed to vary, implying that the cluster frozen structure (with atoms fixed at the coordinates of the isolated crystal) is more stable in the presence of HBr, and that the larger adsorption energy obtained in this fashion is an artifact of the geometry constraints.

Table 3
$HBr/GaAs_2H_5$: binding energies (eV) of frozen and optimized clusters

	DFT	LMP2
Frozen geometry	0.27	0.24
Fully opt. geometry	0.11	0.07

Comparing Fig. 1, depicting the experimental surface geometry, with Fig. 2, where all cluster coordinates have been optimized, we notice a near inversion of the position of the H connected to Ga in relation to the heavy-atom plane, while the other H atoms seem to have rotated around the Ga–As axis, changing the surface H–As–Ga angle, from 109.29° to approximately 90°, similar to that of the interlayer H–As–Ga. Since the presence of HBr on the cluster surface favors the frozen structure over the relaxed one (Fig. 3 shows the completely optimized complex $HBr–GaAs_2H_5$), the approximate agreement, discussed below for the case of MeX of GaAs (110), between experiment and calculations for the binding energies and angle of adsorption obtained via small cluster calculations must be considered fortuitous (see Table 4). Clearly, substantially larger clusters are needed to provide reliable results for molecule–surface interactions.

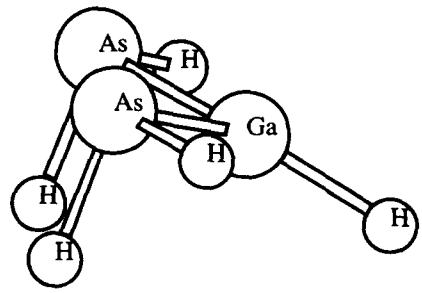

Fig. 1. Geometry of a $GaAs_2H_5$ cluster (small cluster) with coordinates taken from experimental surface measurements.

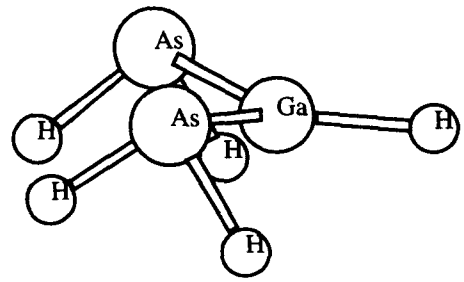

Fig. 2. The same $GaAs_2H_5$ cluster as in Fig. 1, after unrestrained geometry optimization of all coordinates.

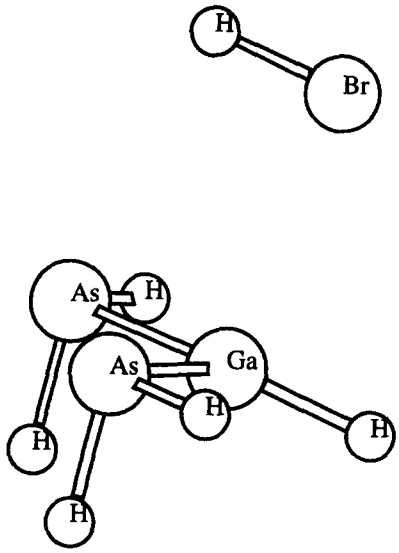

Fig. 3. Geometry of an $HBr/GaAs_2H_5$ complex after unrestrained geometry optimization of all coordinates.

Table 4
$MeX/GaAs_2H_5$: binding energy and angle of adsorption with the surface normal

	PS-LMP2	Experimental (Ref. [17])
Angle (°)	42–49	45–50
Bind. energy (eV)	0.37–0.39	0.42–0.55

3.3.2. *Medium clusters*

$Ga_4As_5H_{13}$ and $Ga_4As_5H_9$ shown in Figs. 4 and 5 respectively are two very different cluster structures with the same number of heavy atoms. The first contains three layers, chosen for the study of interaction of the adsorbate with the inner atoms of the cluster. This cluster is similar to that used by Song et al. in their study of adsorption of alkaline atoms on the same surface [4,26]. The second can be referred to as a "surface cluster", since most of its heavy atoms are arranged in a geometry similar to the first layer of the surface. Note that the key Ga atom bonds are not terminated by hydrogens. However this cluster does not contain the sublayers needed to play a role in long-range interactions with the adsorbate. This cluster was primarily used to search for other orientations of the adsorbate on the surface, since it has a larger number of atoms on the surface and is not

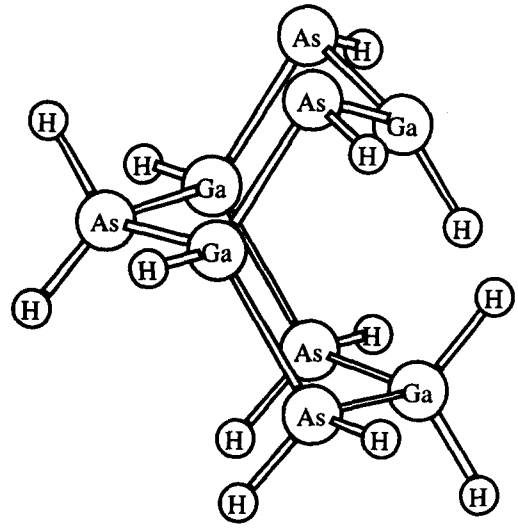

Fig. 4. Geometry of a $Ga_4As_5H_{13}$ cluster (medium cluster), taken with minor modifications from the paper of Song et al. [4,26].

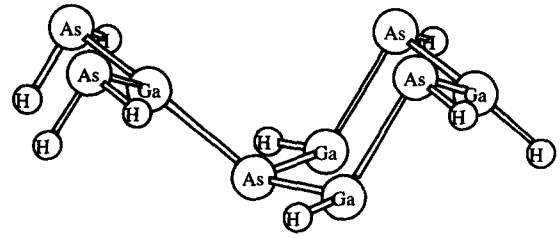

Fig. 5. Geometry of a $Ga_4As_5H_9$ cluster (medium cluster), with heavy atoms arranged in a geometry similar to that of the experimental surface.

too computationally demanding. We performed four geometry optimization calculations, using different initial geometries, to investigate the issue of possible local minima. Figs. 6–9 show the final structures for each optimization and Table 5 contains the energies of each optimized structure. These results demonstrate that there are in fact at least four local minima.

The most stable structure, Geometry 1, has the methyl group pointing towards the As atoms directly connected to the surface gallium binding site. In this most-stable orientation, the halogen atom "sits" close to the top of a surface gallium atom, with the H or methyl group taking a position on top or in between the As atoms directly con-

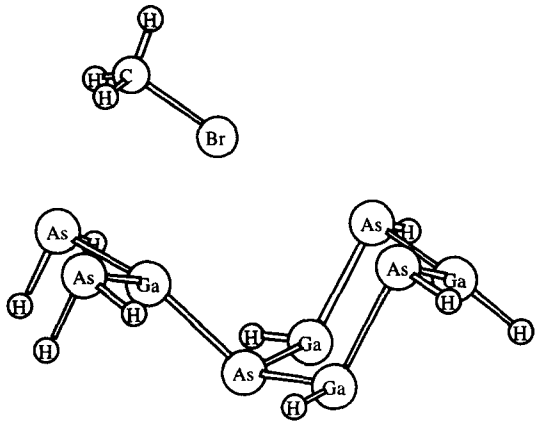

Fig. 6. MeBr/$Ga_4As_5H_9$ complex, in Geometry 1, after geometry optimization of all coordinates.

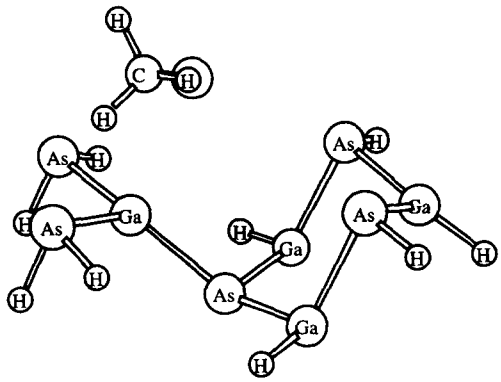

Fig. 7. MeBr/$Ga_4As_5H_9$ complex, in Geometry 2, after geometry optimization of all coordinates.

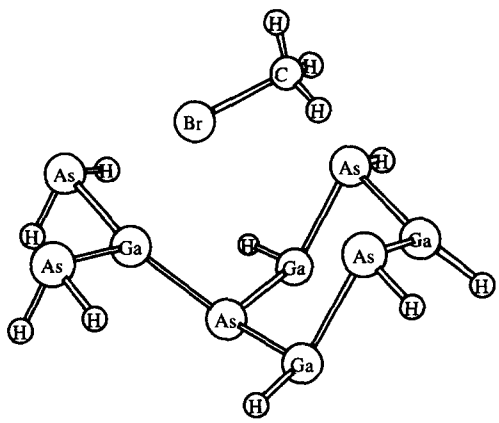

Fig. 8. MeBr/$Ga_4As_5H_9$ complex, in Geometry 3, after geometry optimization of all coordinates.

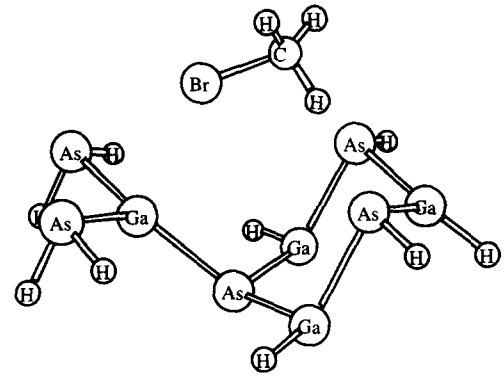

Fig. 9. MeBr/$Ga_4As_5H_9$ complex, in Geometry 4, after geometry optimization of all coordinates.

Table 5
MeBr/$Ga_5As_4H_9$: binding energies for different orientations of the adsorbate. ΔE (eV) corresponds to the difference between the total energy of each geometry and the energy of the most stable structure (1)

Geometry	Total energy $E(h)$	ΔE (eV)
1	−98.83044351305	0.00
2	−98.82571965458	0.13
3	−98.82488842146	0.15
4	−98.82197825809	0.23

nected to the binding Ga. Variation of the orientation of the hydrogens of the methyl group, with regard to the surface, appeared to introduce only small changes on the binding energy or angle of adsorption. In general, conformation (1), with two hydrogens pointing in the direction of the As atoms, was used, since it yielded a slightly larger binding energy. Conformation (2), (see Fig. 10) has one hydrogen pointing to the middle point between the two As atoms, while the other two point away from the surface.

To address the importance of the cluster sublayers, another medium-size cluster was used, which, as stated above, is similar to one of those used by Song and collaborators [4,26]. In their article, they refer to two different molecular formulae for a cluster with same general structure as the one described here, but containing a different number of capping hydrogens. For example, one cluster, $Ga_4As_5H_{12}$, contains an odd numbers of electrons, and does not appear to correctly repre-

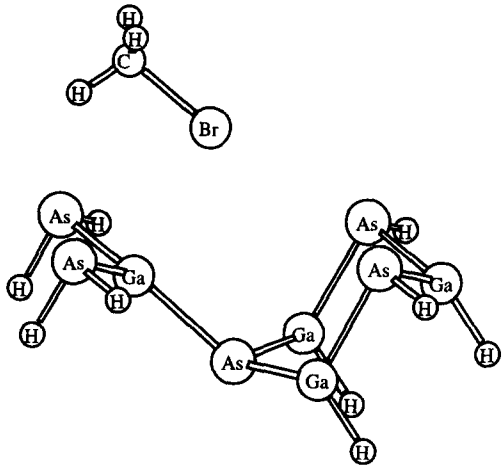

Fig. 10. MeBr/$Ga_4As_5H_9$ complex, in Geometry 1, Conformation 2, after geometry optimization of all coordinates.

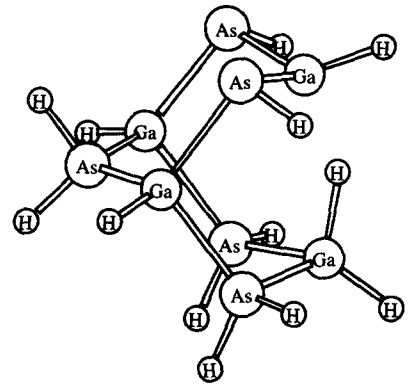

Fig. 11. $Ga_4As_5H_{13}$ cluster, after geometry optimization of all coordinates.

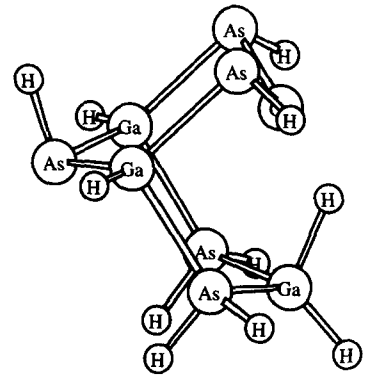

Fig. 12. $Ga_4As_5H_{11}$ cluster, after geometry optimization of all coordinates.

sent the closed-shell surface. Their second cluster, $Ga_4As_5H_{11}$, does contain an even number of electrons, but is missing a key dative-bond resonance structure characteristic of the bulk GaAs crystal. By slightly modifying the latter structure via the addition of two hydrogens, we were able to recover the dative-bond resonance; the resulting $Ga_4As_5H_{13}$ cluster is shown in Fig. 4.

The first step in using the medium clusters involved a search for the global energy minimum for $Ga_4As_5H_9$, $Ga_4As_5H_{13}$, and $Ga_4As_5H_{11}$. The latter cluster is included in our discussion in order to show clearly the effects of a non-resonance cluster in our study. After this minimization in the case of the surface cluster, $Ga_4As_5H_9$, a clear modification occurred in the structure surrounding the Ga atoms; the bonds exhibited a planar distribution, with the disappearance of the surface reconstruction, and a major change in the binding site. Nevertheless, the adsorption energies of HBr on this cluster calculated after full optimization were quite similar to that of the frozen cluster geometry. Regarding the other two cluster structures, the resulting optimized geometries deviated considerably from the initial structure, particularly at the binding site. Figs. 11 and 12 show the two new geometries, which should be compared to Fig. 4. In the case of $Ga_4As_5H_{13}$, note the interaction of the third-layer hydrogen atom with the surface Ga, which pushes the hydrogen directly bonded to it in an upwards direction. Examination of this cluster structure along with the same one in the presence of HBr, also after full optimization, shows that in both cases the surface hydrogen moves down in the presence of the adsorbate. This movement suggests that the surface gallium atom interacts with both the third-layer hydrogen and the bromine atom (Fig. 13).

An even more striking effect was noticed when the non-resonant cluster, $Ga_4As_5H_{11}$, was used; after optimization of the isolated cluster, the surface hydrogen actually detaches from the surface Ga and binds to the near third-layer Ga atom. In the presence of the adsorbate, an optimized geometry was never achieved, with the cluster bonds being broken, but again the surface hydrogen atom moved to the sub-layer, as Fig. 14 shows. This is

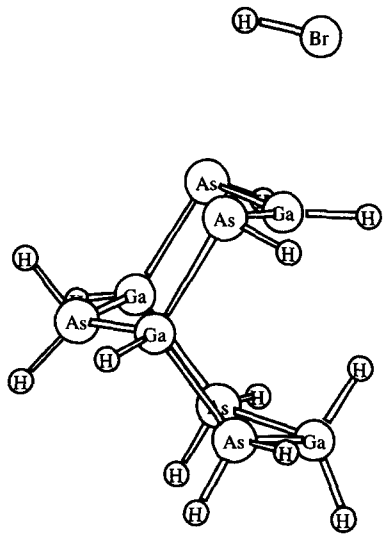

Fig. 13. $HBr/Ga_4As_5H_{13}$ complex, after geometry optimization of all coordinates.

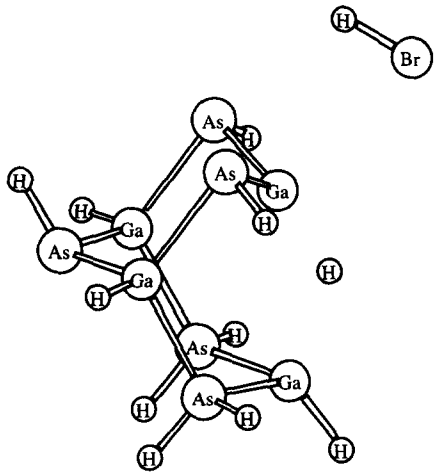

Fig. 14. $HBr/Ga_4As_5H_{11}$ complex, after geometry optimization of all coordinates.

the last structure of the series of geometry iterations preserving the cluster skeleton structure, but still represents a non-bonded adsorbate–cluster system.

3.3.3. *Large clusters*

Having observed the difficulties shown in the smaller clusters described above, our large cluster was designed to avoid these problems to the greatest extent possible. In addition our large cluster contains most of the important features necessary to mimic the real surface from the adsorbate viewpoint. All atoms which are nearest neighbors to the binding site do not contain bonds terminated by hydrogen atoms. In addition, the cluster contains three layers, thus allowing for inclusion of long-range interactions, and according to the results of total geometry optimization for medium clusters, shown above, the binding site should be stable for a three-layer structure.

Due to the long computational time required for the geometry optimization of the large cluster, with or without the adsorbate, calculations were performed using only HBr and MeBr as adsorbates. The results from the geometry optimization of the adsorbates complexed with the $Ga_4As_5H_9$ cluster were used as the starting geometry. Satisfactory results were obtained with the frozen-cluster geometry, optimizing only the coordinates of the adsorbate, and, in our most extensive calculation, a limited surface reconstruction was allowed by letting the three surface atoms closest to the adsorbate move within the $[1\bar{1}1]$ plane. The stability of the surface in regard to our method was confirmed by geometry optimization, which resulted in only small changes from the starting geometry. On the other hand, the surface changed noticeably when the cluster–adsorbate system was optimized.

An important question is the charge distribution of the cluster and the change in this distribution (and of that of the adsorbate) upon the formation of the complex. To address this question, the molecular electrostatic potential and the dipole moment were fit to a set of point charges located on the atom centers [27–29]. Comparing the distribution of charges among the atoms in the uncomplexed systems (bare cluster/isolated MeBr) and the MeBr/cluster complex yielded insight into the electrostatic binding forces between the adsorbate and the surface. Figs. 15–17 display the atomic point charges obtained from the fitting procedure for separated and adsorbed systems.

Important insight can also be obtained by analyzing the cluster before adsorption. As was discussed above, the use of hydrogen to terminate dangling bonds in the cluster significantly disturbs

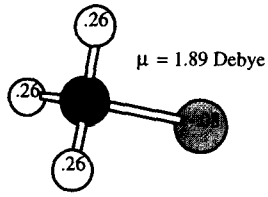

Fig. 15. Electrostatic potential fit charges and dipole moment from B3-LYP calculations on CH_3Br.

the surrounding charge distribution. This effect can be seen by examining pairs of the same kind of atoms with same type of location on the cluster, but with different neighboring atoms and then comparing the point charges assigned to each of them.

For instance, let us compare the charges on the Ga atoms on the third layer. The atom on the left, bound to only one hydrogen, has a charge of 0.37; while the one on the right, bound to two hydrogens, has a net charge of only 0.13. Next, we compare the charge on the second layer Ga atoms, viz. the leftmost atoms, each connected to one hydrogen atom and the rightmost which are fully coordinated within the lattice. The same tendency for smaller positive charge concentration on the Ga atoms with increasing hydrogen ligands is seen. Interestingly, the same effect is not seen in the first layer, where the Ga atoms connected to hydrogen possess larger charge than those bound in the lattice. Note, however, that the first-layer atoms do not participate in the resonance present in the other layers and are connected to only two As atoms, not three. A similar trend is observed for the As atoms, with those bound to hydrogen having a less negative charge, although the effect does not seem as noticeable when only one of the dangling bonds is terminated by hydrogen.

Turning to the adsorption complex, there is a major shift of charge in the methyl bromide upon adsorption; the dipole moment increases from 1.88 to 2.34 Debye, i.e. by about 25%. There is also a transfer of charge from the adsorbate to the cluster of about 0.05 negative charge units. This transfer is probably a consequence of the overlap between the lone electron pair of the bromine and the empty Ga p orbital. Surprisingly the cluster also experiences significant charge redistribution. In Fig. 17, atoms which have gained or lost more

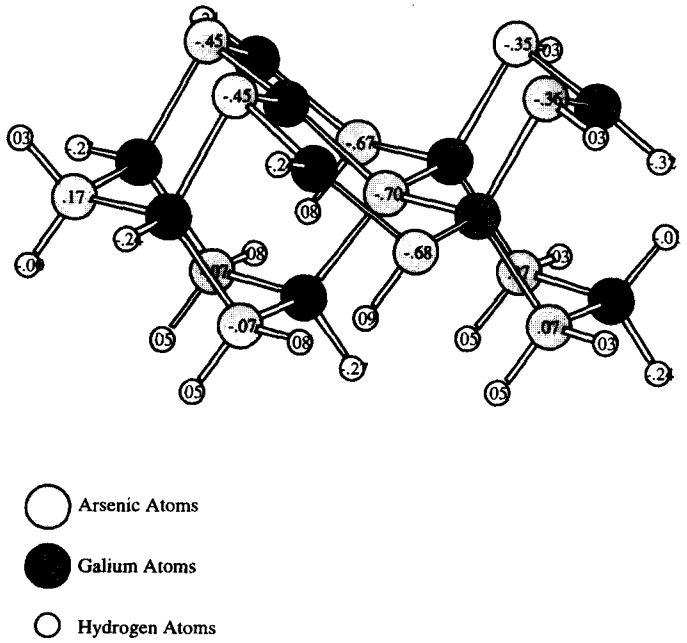

Fig. 16. Electrostatic potential fit charges from B3-LYP calculations on $Ga_{10}As_{10}H_{22}$, using a cluster with surface reconstruction.

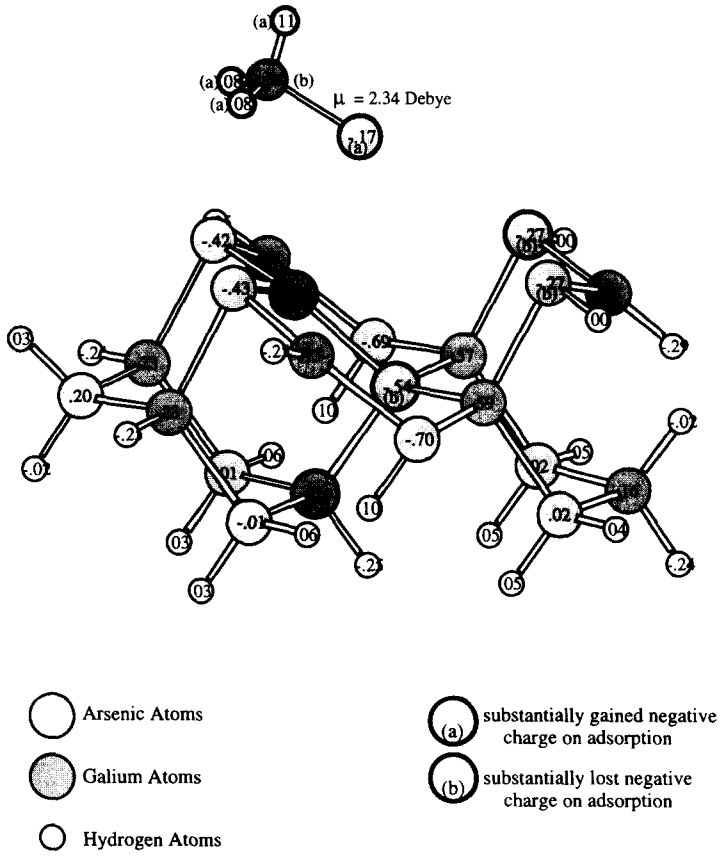

Fig. 17. Electrostatic potential fit charges from B3-LYP calculations on a $CH_3Br/Ga_{10}As_{10}H_{22}$ complex, using a cluster with surface reconstruction. The structure was optimized via a restrained geometry optimization as discussed in the text.

than 0.05 negative charge units on adsorption are highlighted. The charge redistribution affects atoms in all layers, but is most noticeable in the first and second layers. The first-layer Ga and the second-layer As atoms located directly below the C and Br atoms of the adsorbate, have gained and lost, respectively, about 0.15 charge units; this is the largest charge shift in the cluster. This redistribution of charge is nearly the mirror image of that present in the adsorbate and is due to a polarizing electrostatic interaction. This effect is also found in the third layer, where the Ga atom also turns less positive. On the top right of the cluster, electronic charge movement from the arsenic atoms to gallium is observed, probably as a result of the repulsion of the bromine and arsenic lone pairs. Also, the net charge of the group of atoms on the top right diminishes by about 0.1 charge units.

The analysis of the charge redistribution on the cluster brings useful insight with regard to the quality of our cluster. The atoms presenting the largest charge change upon adsorption are the most important in the description of the interaction; the results suggest several reasons for the inclusion of additional atoms to our cluster. First, all atoms with substantial charge shift should not have bonds terminated by hydrogens. Since the third-layer Ga atom on the left and the third-layer As atoms on the right display a measurable amount of transferred charge, a fourth layer should most probably be added to the cluster. In addition, the top right side of the cluster seems to interact strongly with the adsorbate and since the Ga and As atoms are

all at present terminated by hydrogens, additional Ga and As atoms should be added in this location.

3.4. Comparative results for all clusters

In the previous sections, a qualitative description of the various clusters and calculations used in this study were presented. Here, we summarize and compare the quantitative results obtained for the adsorbate–surface geometries and the energetics of binding. We characterize the binding of both the hydride and methyl halogens by three quantities: the distance between the halogen and the closest surface atom, the adsorption angle between the adsorbate and the surface, and the binding energy of the adsorbate to the surface.

Consider first the geometry of the adsorbate in the binding site. Table 6 presents the distance between the halogen of the adduct and the closest atom on the surface, Ga, which we will refer as h; the distances vary from a minimum of 2.7 Å to a maximum of 3.5 Å. The shortest distances are obtained with the small cluster. Both medium clusters, despite the difference in structure, yield essentially identical results, viz. the large values of h, while the result for the large cluster is intermediate between the small and medium clusters. The distance h presents exactly the same trend for all clusters, becoming larger as the diameter of the halogen increases. Note also that the MeX adsorbates display slightly smaller h values than do the HX species, probably due to the larger dipole moment of the methyl halides in comparison with the hydrogen halides.

Table 6
Distance between X and nearest Ga atoms (Å)

	$GaAs_2H_5$	$Ga_4As_5H_9$	$Ga_4As_5H_{13}$	$Ga_{10}As_{12}H_{22}$
HCl	2.8	3.3	3.2	–
HBr	3.0	3.4	3.3	3.2
HI	3.1	3.5	3.5	–
MeCl	2.7	2.9	2.9	–
MeCl(2)	2.8	–	–	–
MeBr	2.9	3.1	3.1	3.0
MeBr(2)	2.9	3.1	–	–
MeI	3.0	3.3	3.3	–
MeI(2)	3.0	–	–	–

The adsorption angle is defined as the angle between the C–X or H–X bond in the adsorbate and the surface normal. As can be seen from Table 7, this angle systematically increases as the size of the cluster is increased. This trend could have been predicted, since long-range dipole–dipole interactions of adsorbate and the cluster sublayers are expected. In addition, the results on the orientation of the methyl halides on the cluster $Ga_4As_5H_9$, referred to as (2) in Table 7 (see, for example, Fig. 10). Our results for the adsorption angles vary not only with the cluster, but also with the adsorbate, in agreement with the experimental results. Note also that while the adsorption angle seems to decrease with the size of the halogen in the hydrogen halides, the opposite trend is observed for the methyl halides. The polarizability of the halogens appears to explain these two apparently contradictory trends.

According to Table 8, iodine, having the largest covalent radius, is the most polarizable among the listed halogens and therefore will bind more strongly with Ga, thus increasing the dipole moment of the adduct, and making the hydrogen or methyl group even more willing to interact with the lone electron pairs of the As atoms. From the charge distribution results described above, the As atoms have excess negative charge after the adsorp-

Table 7
Angle (°) of adsorption with surface normal

	$GaAs_2H_5$	$Ga_4As_5H_9$	$Ga_4As_5H_{13}$	$Ga_{10}As_{12}H_{22}$	Exp. Ref. [17]
HCl	52	75	68	–	–
HBr	51	63	64	66	–
HI	45	59	66	–	–
MeCl	42	45	44	–	45±5
MeCl(2)	39	–	–	–	–
MeBr	46	49	49	55	45±5
MeBr(2)	43	48	–	–	–
MeI	49	56	57	–	55±5
MeI(2)	47	–	–	–	–

Table 8
Covalent radius of halogens

	Cl	Br	I
Covalent radius (Å)	0.99	1.14	1.33

tion due to transfer of a small amount of electronic charge from the halogen to the Ga atom. According to this argument, the angle between the surface normal and the adsorbate should increase when going from adducts containing chlorine to those containing iodine, a result which is, in fact, seen for the case of the methyl halides. It does not apply to the hydrogen halides, though, and again we can use the size trend of the halogens for an explanation. The bond distances between the carbon atom and the halogens in the methyl halides are roughly 0.5 Å larger than those between hydrogen and the halogens in the hydrogen halides; this makes the screening of the positive charge on the hydrogen more likely to occur than for the relatively more distant and more polarizable methyl group. And since the screening effect increases with the size of the halogen, the larger the halogen, the smaller the angle of the adsorbate with the surface normal, as is observed in our calculations.

Finally, the binding energies of H*X* and Me*X* on all clusters can be found in Table 9 and 10, respectively. The binding energy of the hydrogen halides is smaller than that of the methyl halides by an average of 0.1 eV. This suggests that a large part of the binding occurs due to polarization, and since the larger Me*X* molecules have a more diffuse electron cloud, the adjustment of its charge to an external field is more effective, increasing the effective electrostatic interaction and, therefore, the binding energy.

Note that the values for the Hartree–Fock (HF) binding energies are much smaller than the experimental ones, with the exception of those obtained with $GaAs_2H_5$, where interactions with capping hydrogens near the binding site result in attractive forces absent in the infinite surface. It is clear that even qualitatively reasonable results for binding energies require the inclusion of electron correlation in the calculations.

We next consider the DFT calculations. The B3LYP functional gives significantly larger binding energies and is hence in better agreement with experiment than the BLYP results, which are substantially in error. This is in accord with the results discussed above concerning the superiority of functionals derived from the adiabatic connection formulas, which contain an admixture of Hartree–Fock exchange. It should be noted, however, that an important implication of this observation is that plane-wave based DFT methods cannot be expected to provide quantitative results for binding energies of molecules to surfaces, as these computational methods have severe difficulty with the inclusion of nonlocal exchange terms.

Finally, we examine the LMP2 results. There is a reasonably good correlation between the LMP2 and B3LYP results, with the latter displaying a small quantitative superiority for the final, large cluster value (this may in part be due to the fact that the geometry was optimized using the B3LYP method; the LMP2 binding energy at its own equilibrium binding energy will be larger than that

Table 9
Binding energies (eV) of H*X* on the small, medium and large clusters

		Frozen				Reconstruction	
		HF	B3LYP	LMP2	BLYP	B3LYP	LMP2
HCl on	$GaAs_2H_5$	0.12	0.29	0.26	0.20		
	$Ga_4As_5H_9$	0.06	0.15	0.16	–	0.13	–
	$Ga_4As_5H_{13}$	0.06	0.14	0.15	–	–	–
HBr on	$GaAs_2H_5$	0.09	0.27	0.24	0.16		
	$Ga_4As_5H_9$	0.01	0.14	0.16	–	0.13	0.16
	$Ga_4As_5H_{13}$	0.03	0.12	0.13	–	0.16	0.15
	$Ga_{10}As_{12}H_{22}$	−0.06	0.15	0.18	–	0.14	0.20
HI on	$GaAS_2H_5$	0.06	0.28	0.24	0.14	–	–
	$Ga_4As_5H_9$	−0.05	0.15	0.18	–	–	–
	$Ga_4As_5H_{13}$	0.01	0.11	0.13	–	–	–

Table 10
Binding energies (eV) of CH_3X on the small, medium and large clusters

	Frozen				Reconstruction	
	HF	B3LYP	LMP2	BLYP	B3LYP	LMP2
CH_3Cl (Experimental value: 0.42 eV – Ref. [17]) on						
$GaAS_2H_5$	0.22	0.42	0.39	0.29	—	—
$Ga_4As_5H_9$	0.05	0.21	0.22	0.08	—	—
$Ga_4As_5H_{13}$	0.10	0.21	0.22	–	—	—
CH_3Br (Experimental value: 0.47 (eV – Ref. [17]) on						
$GaAs_2H_5$	0.19	0.43	0.38	0.27	–	–
$Ga_4As_5H_9$	0.02	0.24	0.24	0.07	0.24	0.29
$Ga_4As_5H_{13}$	0.09	0.21	0.22	–	–	–
$Ga_{10}As_{10}H_{24}$	−0.06	0.22	0.28	–	0.33	0.27
CH_3I (Experimental value: 0.55 eV – Ref. [17]) on						
$GaAs_2H_5$	0.16	0.42	0.37	0.24	–	–
$Ga_4As_5H_9$	0.01	0.24	0.25	0.05	–	–
$Ga_4As_5H_{13}$	0.06	0.21	0.22	–	–	–

reported here). At this point, both methods have to be considered as reasonable (if not high precision) methods for the determination of molecule–surface binding energies.

A few general observations concerning both the LMP2 and B3LYP results can be made. First, after the artificial results of the small cluster, binding energy increases with cluster size (although not dramatically). Secondly, the surface reconstruction contributes to enhancement of the binding energy. Thirdly, the results suggest that each method is missing some systematic component of the energy, leading to underestimation of binding.

In the case of DFT, one possible missing component is the dispersion energy, which it is well known is not properly represented by DFT methods. For the LMP2, higher order terms in the perturbation series may be required. Finally, larger basis sets may need to be used with both approaches. These issues will be investigated in future work.

4. Conclusion

We have shown that it is possible, using modern quantum chemical methods and PSGVB, to calculate the binding energy of an adsorbate molecule to a surface with reasonable accuracy, by careful construction of the cluster to resemble the actual crystal surface and the employment of correlated electronic structure methods. The error in the binding energy, ~0.15 eV for the best (B3LYP) calculation to date, is in fact comparable to errors obtained with this method in small molecule test cases [7]. In addition to computing binding energy, a great deal of physical insight into the binding interactions was obtained from an analysis of the geometry optimizations and charge distribution of the cluster and cluster–adsorbate complex.

Our accuracy, 35% too low, is still not entirely satisfactory, since the computed dative bond energy is small, 0.47 eV. To obtain more accurate results, higher level ab initio methods and a larger basis set will be necessary. Conventional methods of this type, such as CCSD(T), are impractical, given the size of the system required to obtain reasonable results and the scaling of N^7 of such methods, with N the number of atoms in the system. However, we have recently completed the development of a multireference LMP2 method, GVB-LMP2, which in preliminary tests displays accuracy comparable to CCSD(T) but scales in the N^2–N^3 range. Only a small part of the surface–adsorbate cluster will need to be treated at the GVB level, viz. that directly involved in the dative

bond; the remainder can be treated at the LMP2 level. A calculation with this method will result in an increased binding energy and should lead to near-chemical accuracy.

Acknowledgements

R.O. and P.H. Lu would like to thank DOE, contract DE-F602-9OER14104, for support of this research. R.F. and S.B. thank the Department of Energy, Grant DE-FG02-90ER14162, for support.

References

[1] Per E.M. Siegbahn, Surf. Sci. 269/270 (1992) 276.
[2] N.U. Zhanpeisov, E.A. Paukshtis, G.M. Zhidomirov, V.A. Zakharov, Catal. Lett. 29 (1994) 209.
[3] G.S. Khoo, C.K. Ong, Phys. Rev. B 50 (1994) 10796.
[4] K.M. Song, D.C. Khan, A.K. Ray, Phys. Rev. 49 (1994) 1818.
[5] P. Hohenberg, W. Kohn, Phys. Rev. B 136 (1964) 864.
[6] W. Kohn, L.J. Sham, Phys. Rev. A 140 (1965) 1133.
[7] A.D. Becke, J. Chem. Phys. 98 (1993) 5648.
[8] A.D. Becke, J. Chem. Phys. 98 (1993) 1372.
[9] A.D. Becke, J. Chem. Phys. 97 (1992) 9173.
[10] B. Hammer, Y. Morikawa, J.K. Nørskov, Phys. Rev. Lett. 76 (1996) 214.
[11] M.N. Ringnalda, J.M. Langlois, R.B. Murphy, B.H. Greely, C. Cortis, T.V. Russo, B. Marten, R.E. Donnelly Jr., W.T. Pollard, Y. Cao, R.P. Muller, D.T. Mainz, J.R. Wright, Gregory H. Miller, W.A. Goddard III, R.A. Friesner, PS-GVB, Schroedinger Inc., 1996.
[12] H. Yong, T.C. Caves, J. Whitten, J. Am. Chem. Soc. 116 (1994) 8200.
[13] G. Te Velde, A.J. Baerends, Chem. Phys. 177 (1993) 399.
[14] H. Burghraef, A.J. Jansen, R. Van Santen, Chem. Phys. 177 (1993) 407.
[15] K. Neyman, N. Rösch, Chem. Phys. 177 (1993) 561.
[16] J.L. Whitten, Chem. Phys. 177 (1993) 387.
[17] P.H. Lu, P.J. Lasky, Q.Y. Yang, Y. Wang, R.M. Osgood, Jr., J. Chem. Phys. 101 (1994) 10145.
[18] P.J. Lasky, P.H. Lu, M.X. Yang, R.M. Osgood, Jr., B.E. Bent, P.A. Stevens, Surf. Sci. 336 (1995) 140.
[19] P.H. Lu, P.J. Lasky, Q.Y. Yang, R.M. Osgood, Jr., Chem. Phys. 205 (1996) 143.
[20] M.J. Frisch, G.W. Trucks, M. Head-Gordon, P.M.W. Gill, M.W. Wong, J.B. Foresman, B.G. Johnson, H.B. Schlegel, M.A. Robb, E.S. Replogle, R. Gomperts, J.L. Andres, K. Raghavachari, J.S. Binkley, C. Gonzalez, R.L. Martin, D.J. Fox, D.J. Defrees, J. Baker, J.J.P. Stewart, J.A. Pople, Gaussian 92, Revision E.1, Gaussian Inc., 1992.
[21] S. Saebo, W. Tong, P. Pulay, J. Chem. Phys. 98 (1993) 2170.
[22] R.B. Murphy, M.D. Beachy, M.N. Ringnalda, R.A. Friesner, J. Chem. Phys. 103 (1995) 1481.
[23] S. Saebo, P. Pulay, J. Chem. Phys. 86 (1984) 914.
[24] C. Lee, W. Yang, R.G. Parr, Phys. Rev. B 37 (1988) 785.
[25] W.R. Wadt, P.J. Hay, J. Chem. Phys. 82 (1985) 284.
[26] K.M. Song, A.K. Ray, Phys. Rev. 50 (1994) 14255.
[27] L.E. Chirlian, M.M. Francl, J. Comput. Chem. 8 (1990) 894.
[28] R.J. Woods, M. Khalil, W. Pell, S.H. Moffat, V.H. Smith, Jr., J. Comput. Chem. 11 (1990) 297.
[29] C.M. Breneman, K.B. Wiberg, J. Comput. Chem. 11 (1990) 361.